

termolecular contacts other than those noted above for SbCl_3dmit .

The single-crystal X-ray study reported above thus provides further support for the solid-state vibrational data assignments reported earlier. As was the case for SeBr_2tmtu and AsCl_3dmit , there was no clear evidence of bridging in the solid-state spectra of SbCl_3dmit .

Acknowledgment. D.J.W. wishes to thank the Strosacker Foundation of Midland, Mich., for partial support of this research.

Registry No. SbCl_3dmit , 70198-09-3.

Supplementary Material Available: Listing of observed and calculated structure factors (5 pages). Ordering information is given on any current masthead page.

Contribution from the Guelph-Waterloo Centre for Graduate Work in Chemistry, Waterloo Campus, University of Waterloo, Waterloo, Ontario, Canada N2L 3G1, and Istituto di Chimica Inorganica ed Generale, Università di Torino, Torino, Italy

Chemistry of Multisite-Bound Ligands: Crystal and Molecular Structure of $\text{HRu}_3(\text{CO})_8(\text{C}\equiv\text{C}-t\text{-Bu})(\text{PPh}_2\text{OEt})$

Arthur J. Carty,*^{1a} Shane A. MacLaughlin,^{1a}
Nicholas J. Taylor,^{1a} and Enrico Sappa^{1b}

Received May 11, 1981

One goal of our current research programs is to investigate the chemical reactivity associated with the multisite coordination of unsaturated ligands to several metal atoms in metal carbonyl clusters.^{2,3} In attempts to establish distinct patterns of reactivity for cluster-bound ligands, the polynuclear μ -acetylido compounds serve as particularly useful models since a progression of bonding modes, $\mu_2\text{-}\eta^2$,⁴ $\mu_3\text{-}\eta^2$,^{5,6} and $\mu_4\text{-}\eta^2$,⁷ is accessible, and furthermore the problem of ligand mobility frequently associated with other ligands such as CO is largely circumvented.⁸ In studies relating to the susceptibility of $\mu_3\text{-}\eta^2$ -acetylides to nucleophilic attack by uncharged ligands, a number of substitution products derived via carbonyl displacement from the neutral hydride $\text{HRu}_3(\text{CO})_9(\text{C}\equiv\text{C}-t\text{-Bu})$ ⁵ and the related "open" phosphide-bridged trimer $\text{Ru}_3(\text{CO})_9(\text{C}\equiv\text{CR})(\text{PPh}_2)(\text{R} = t\text{-Bu}, i\text{-Pr})$ ⁶ have been characterized. Current interest in such derivatives⁹ prompts us to report an accurate determination of the molecular structure of $\text{HRu}_3(\text{CO})_8(\text{C}\equiv\text{C}-t\text{-Bu})(\text{PPh}_2\text{OEt})$.

Table I. Crystal Data and Intensity Collection

formula	$\text{C}_{28}\text{H}_{25}\text{O}_9\text{PRu}_3$
mol wt	839.69
cryst system, space group	triclinic, $P\bar{1}$
cell	$a = 9.141(1)$, $b = 11.706(2)$, $c = 15.057(2)$ Å; $\alpha = 96.73(1)$, $\beta = 84.36(1)$, $\gamma = 100.31(1)^\circ$
Z	2
d_{measd}	1.78 g cm ⁻³
d_{calcd}	1.778 g cm ⁻³
V	1568.1(4) Å ³
F(000)	824
T	22 ± 1 °C
radiation	graphite-monochromated Mo K α ($\lambda = 0.71073$ Å)
diffractometer	Syntex P2 ₁
scan type	θ -2 θ
scan speed	variable (2-29.3° min ⁻¹)
scan width	[2 θ (Mo K α_1) - 0.8°] → [2 θ (Mo K α_2 + 0.8°)]
background	stationary counter-stationary crystal before and after each scan
reflectns measd	4136 ($2\theta < 45^\circ$)
reflectns obsd	3538 ($I \geq 3\sigma(I)$)
$\mu(\text{Mo K}\alpha)$	14.93 cm ⁻¹
R	0.024
R_w	0.028

Table II. Fractional Atomic Coordinates ($\times 10^4$) for $\text{HRu}_3(\text{CO})_8(\text{C}_2-t\text{-Bu})(\text{P}(\text{OEt})\text{Ph}_2)$

	x	y	z
Ru(1)	199.2 (4)	4239.5 (3)	3134.4 (2)
Ru(2)	688.8 (4)	1924.5 (3)	2672.4 (2)
Ru(3)	2912.5 (4)	3645.0 (3)	3468.3 (3)
P	1950.4 (12)	448.6 (9)	2078.5 (7)
O(1)	-1802 (4)	1108 (3)	1455 (3)
O(2)	-820 (5)	719 (4)	4296 (2)
O(3)	196 (6)	6790 (4)	3911 (3)
O(4)	-1769 (4)	4197 (4)	1612 (3)
O(5)	-2376 (5)	3151 (4)	4387 (3)
O(6)	5632 (4)	2670 (4)	2604 (4)
O(7)	2498 (5)	2124 (4)	5025 (3)
O(8)	4853 (6)	5873 (4)	4262 (3)
O(9)	3068 (3)	702 (3)	1200 (2)
C(1)	-875 (5)	1398 (4)	1931 (3)
C(2)	-256 (5)	1130 (4)	3680 (3)
C(3)	214 (6)	5859 (5)	3601 (4)
C(4)	-1050 (5)	4228 (4)	2198 (4)
C(5)	-1415 (6)	3532 (5)	3916 (4)
C(6)	4598 (6)	3017 (4)	2937 (4)
C(7)	2647 (6)	2670 (5)	4435 (4)
C(8)	4126 (7)	5057 (5)	3986 (4)
C(9)	1782 (4)	3351 (4)	2220 (3)
C(10)	2373 (4)	4471 (4)	2290 (3)
C(11)	3201 (5)	5388 (4)	1716 (3)
C(12)	4776 (6)	5163 (6)	1465 (5)
C(13)	3242 (9)	6612 (5)	2180 (4)
C(14)	2419 (7)	5250 (6)	853 (4)
C(15)	2791 (7)	1374 (5)	518 (4)
C(16)	4160 (10)	1570 (7)	-96 (5)
C(17)	758 (5)	-914 (4)	1699 (3)
C(18)	-424 (5)	-1412 (4)	2256 (4)
C(19)	-1322 (6)	-2448 (5)	1970 (4)
C(20)	-1086 (7)	-2978 (5)	1118 (4)
C(21)	77 (8)	-2497 (5)	560 (4)
C(22)	1010 (6)	-1462 (4)	841 (3)
C(23)	3215 (4)	-44 (4)	2752 (3)
C(24)	2700 (6)	-453 (4)	3571 (3)
C(25)	3654 (7)	-854 (5)	4074 (4)
C(26)	5101 (6)	-860 (5)	3776 (4)
C(27)	5636 (6)	-464 (5)	2962 (4)
C(28)	4701 (5)	-56 (4)	2439 (4)
H(1)	1383 (50)	4199 (39)	3988 (31)

Experimental Section

The synthesis of the title compound and a wide variety of substitution products will be described in detail elsewhere.¹⁰ Crystals

- (1) (a) Guelph-Waterloo Centre. (b) Università di Torino.
- (2) (a) Carty, A. J.; Mott, G. N.; Taylor, N. J.; Yule, J. E. *J. Am. Chem. Soc.* **1978**, *100*, 3051. (b) Carty, A. J.; Ferguson, G.; Khan, M. A.; Mott, G. N.; Roberts, P. J.; Taylor, N. J.; *J. Organomet. Chem.* **1978**, *149*, 345. (c) Carty, A. J.; Mott, G. N.; Taylor, N. J.; *J. Organomet. Chem.* **1979**, *182*, C69. (d) Carty, A. J. *Adv. Chem. Ser.*, in press.
- (3) (a) Osella, D.; Sappa, E.; Tiripicchio, A.; Tiripicchio-Camellini, M. *Inorg. Chim. Acta* **1979**, *34*, L289. (b) Sappa, E.; Tiripicchio, A.; Tiripicchio-Camellini, M.; *J. Chem. Soc., Chem. Commun.* **1979**, 254. (c) Aime, S.; Milone, L.; Sappa, E.; Tiripicchio, A.; Tiripicchio-Camellini, M. *Inorg. Chim. Acta* **1978**, *32*, 163.
- (4) Smith, W. F.; Yule, J. E.; Taylor, N. J.; Paik, H. N.; Carty, A. J. *Inorg. Chem.* **1977**, *16*, 1593.
- (5) Sappa, E.; Gambino, O.; Milone, L.; Cetini, G. *J. Organomet. Chem.* **1972**, *39*, 169.
- (6) Carty, A. J.; MacLaughlin, S. A.; Taylor, N. J. *J. Organomet. Chem.* **1981**, *204*, C27.
- (7) Carty, A. J.; MacLaughlin, S. A.; Taylor, N. J. *J. Am. Chem. Soc.* **1981**, *103*, 2456.
- (8) Aime, S.; Gambino, O.; Milone, L.; Sappa, E.; Rosenberg, E. *Inorg. Chim. Acta* **1975**, *15*, 53.
- (9) Jangala, C.; Rosenberg, E.; Skinner, D.; Aime, S.; Milone, L.; Sappa, E. *Inorg. Chem.* **1980**, *19*, 1571.

Table III. Anisotropic Thermal Parameters ($\times 10^4$) for $\text{HRu}_3(\text{CO})_8(\text{C}_2\text{-}t\text{-Bu})(\text{P}(\text{OEt})\text{Ph}_2)^a$

	β_{11}	β_{22}	β_{33}	β_{12}	β_{13}	β_{23}
Ru(1)	121.9 (6)	64.2 (3)	39.6 (2)	25.7 (3)	-0.3 (2)	6.1 (2)
Ru(2)	94.2 (5)	53.2 (3)	37.3 (2)	8.3 (3)	-8.0 (2)	7.1 (2)
Ru(3)	128.1 (6)	65.8 (3)	46.7 (2)	8.2 (3)	-29.4 (3)	4.2 (2)
P	92.4 (14)	54.0 (9)	34.2 (5)	10.6 (9)	-3.9 (7)	9.2 (5)
O(1)	134 (5)	135 (4)	65 (2)	-7 (4)	-39 (3)	11 (2)
O(2)	235 (7)	134 (4)	54 (2)	36 (4)	40 (3)	38 (2)
O(3)	389 (11)	88 (4)	82 (3)	77 (5)	3 (4)	-17 (3)
O(4)	167 (6)	142 (4)	80 (2)	18 (4)	-42 (3)	32 (3)
O(5)	224 (7)	179 (5)	79 (3)	41 (5)	64 (4)	45 (3)
O(6)	127 (6)	116 (4)	163 (4)	26 (4)	8 (4)	12 (3)
O(7)	293 (8)	141 (5)	71 (2)	19 (5)	-56 (4)	40 (3)
O(8)	351 (10)	110 (4)	108 (4)	-51 (5)	-106 (5)	-8 (3)
O(9)	135 (4)	90 (3)	40 (2)	32 (3)	9 (2)	21 (2)
C(1)	111 (6)	69 (4)	46 (2)	9 (4)	2 (3)	13 (2)
C(2)	128 (7)	74 (4)	55 (3)	26 (4)	-3 (4)	2 (3)
C(3)	190 (9)	94 (5)	52 (3)	46 (5)	1 (4)	2 (3)
C(4)	109 (7)	78 (4)	63 (3)	18 (4)	4 (4)	17 (3)
C(5)	164 (8)	108 (5)	55 (3)	42 (5)	7 (4)	13 (3)
C(6)	132 (8)	72 (4)	93 (4)	-8 (5)	-26 (4)	8 (3)
C(7)	190 (9)	95 (5)	64 (3)	16 (5)	-49 (4)	13 (3)
C(8)	215 (10)	98 (5)	69 (3)	1 (6)	-54 (5)	5 (3)
C(9)	86 (5)	64 (4)	31 (2)	19 (4)	-8 (2)	-2 (2)
C(10)	98 (6)	61 (4)	37 (2)	15 (4)	-6 (3)	6 (2)
C(11)	129 (7)	64 (4)	50 (2)	2 (4)	-2 (3)	10 (2)
C(12)	150 (9)	136 (7)	112 (5)	11 (6)	29 (6)	56 (5)
C(13)	375 (16)	63 (5)	70 (4)	-25 (7)	28 (7)	8 (3)
C(14)	205 (11)	147 (7)	65 (3)	-24 (8)	-14 (5)	52 (4)
C(15)	267 (12)	124 (6)	51 (3)	70 (7)	28 (5)	35 (3)
C(16)	422 (21)	190 (10)	81 (4)	126 (11)	90 (8)	75 (6)
C(17)	118 (6)	60 (4)	43 (2)	24 (4)	-21 (3)	3 (2)
C(18)	130 (7)	78 (4)	63 (3)	-6 (4)	3 (4)	-0 (3)
C(19)	158 (8)	85 (5)	92 (4)	-16 (5)	-20 (5)	13 (4)
C(20)	202 (9)	81 (5)	80 (4)	-5 (6)	-54 (5)	4 (3)
C(21)	285 (12)	85 (5)	58 (3)	8 (6)	-47 (5)	-9 (3)
C(22)	205 (9)	81 (4)	47 (3)	15 (5)	-14 (4)	4 (3)
C(23)	98 (6)	58 (3)	39 (2)	9 (4)	-8 (3)	6 (2)
C(24)	142 (8)	107 (5)	47 (3)	36 (5)	-2 (4)	24 (3)
C(25)	210 (10)	126 (6)	49 (3)	59 (6)	-16 (4)	24 (3)
C(26)	177 (9)	109 (5)	72 (3)	46 (6)	-43 (5)	17 (3)
C(27)	114 (8)	130 (6)	80 (4)	40 (5)	-14 (4)	24 (4)
C(28)	120 (7)	99 (5)	55 (3)	21 (4)	-1 (4)	20 (3)

^a B_{iso} for H(1): 6 (1) \AA^2 .

of $\text{HRu}_3(\text{CO})_8(\text{C}_2\text{-}t\text{-Bu})(\text{PPh}_2\text{OEt})$ from heptane are irregular, yellow prisms, mp 159 °C. Preliminary Weissenberg and precession photographs revealed no systematic absences; Laue symmetry $\bar{1}$ was ensured, leaving space groups $P\bar{1}$ or $P\bar{1}$ as alternatives. The latter was shown to be correct by the successful refinement of the structure.

Collection and Reduction of X-ray Data. A suitable crystal of dimensions $0.24 \times 0.26 \times 0.27$ mm was selected for data collection, set on a glass fiber and brass pin with epoxy cement, and attached to a Supper goniometer head for mounting on the diffractometer (Syntex P2₁). After careful centering, polaroid rotation photographs were used to locate 15 reflections of suitable intensity widely dispersed in reciprocal space. The Syntex autoindexing and cell refinement package was then used to refine accurate cell parameters from the setting angles of these 15 reflections and to define the orientation matrix. Crystal data and details pertinent to the collection of intensities are listed in Table I. The variation in intensity of two standard reflections (316; 401), repeatedly counted after every 100 observations, was less than 2%. After data collection, intensities were corrected for Lorentz and polarization effects, then converted to F_o in the normal way. With a small, equidimensional crystal and a small value of μ , no absorption correction was necessary.

Solution and Refinement of the Structure. A Patterson map readily revealed the positions of three independent ruthenium atoms. Full-matrix least-squares refinement, Fourier, and difference Fourier methods were used to locate the remaining nonhydrogen atoms. Isotropic least-squares refinement of nonhydrogen atoms yielded an R value of 0.074. After two cycles of refinement with anisotropic coefficients, R had dropped to 0.032 with none of the atoms showing evidence of unusual behavior. A difference Fourier calculated at this

stage allowed the unequivocal assignment of reasonable positions for all hydrogen atoms including the hydride, located in a bridging position between Ru(2) and Ru(3). In final cycles of refinement, the hydride hydrogen atom position and isotropic thermal parameter were allowed to vary while other hydrogen atoms were held in fixed positions. The final R and R_w values were 0.024 and 0.028. In a final difference map, the background electron density was at the level of 0.3 e \AA^{-3} . On this scale a typical hydrogen atom appears as a peak of height 0.45 e \AA^{-3} .

The function minimized in least-squares refinements was $\sum w(|F_o| - |F_c|)^2$ with $w^{-1} = 1.67 - 0.02|F| + 0.00033|F|^2$ in the final weighting. The residuals R and R_w were defined as $R = \sum ||F_o| - |F_c|| / \sum |F_o|$ and $R_w = [\sum w(|F_o| - |F_c|)^2 / \sum w|F_o|^2]^{1/2}$. Atomic scattering factors used were those listed in ref 11 with the exception of hydrogen where the data of Stewart¹² were used. Computer programs used are described elsewhere.^{2a} A listing of observed and calculated structure factors is available as supplementary material. Atomic positions for heavy atoms and the bridging hydrogen are listed in Table II with anisotropic thermal parameters in Table III. A compilation of important bond lengths and angles is given in Table IV. Supplementary Tables S1 (hydrogen atom positions and B 's) and S2 (remaining bond lengths and angles) are available.

Results and Discussion

An ORTEP II plot of the molecular structure drawn to illustrate both the acetylde-metal interactions and the bridging

(10) Carty, A. J.; Sappa, E.; MacLaughlin, S. A., unpublished results.

(11) "International Tables for X-ray Crystallography"; Kynoch Press: Birmingham, England, 1974; Vol. IV.

(12) Stewart, R. F.; Davidson, E. R.; Simpson, W. J. *J. Chem. Phys.* **1965**, *42*, 3175.

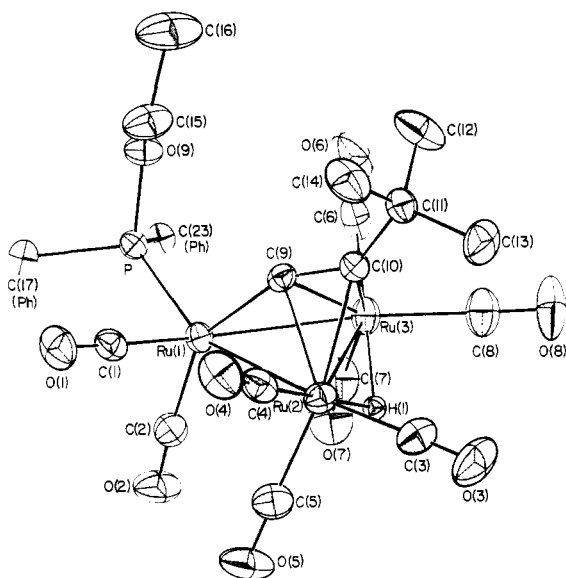


Figure 1. View of the molecule $\text{HRu}_3(\text{CO})_8(\text{C}\equiv t\text{-Bu})(\text{PPh}_2\text{OEt})$. Only one carbon atom of each phenyl ring is illustrated, and with the exception of the bridging hydride no hydrogen atoms are shown.

hydride is shown in Figure 1. The basic structure is similar to that of $\text{HRu}_3(\text{CO})_9(\text{C}\equiv\text{C}-t\text{-Bu})(\text{PPh}_2)$,¹³ with the hydride bridging one edge of an almost equilateral triangle of ruthenium atoms. The phosphine is coordinated to Ru(1) (the ruthenium atom σ bonded to the organic ligand), as predicted from solution ¹³C NMR studies,⁹ and occupies a radial site approximately trans to the Ru(1)–Ru(2) bond. The Ru–Ru bond lengths average 2.820 Å, a typical value for Ru–Ru single bonds in closed triangular clusters,¹⁴ with no bond length differing by more than ± 0.021 Å from the mean. There is a very interesting comparison with the parent molecule $\text{HRu}_3(\text{CO})_9(\text{C}\equiv\text{C}-t\text{-Bu})$ ¹³ inasmuch as the length of the Ru–Ru vector bridged by the hydride is essentially the same in both molecules (2.7988 (5) vs. 2.795 (1) Å in $\text{HRu}_3(\text{CO})_9(\text{C}\equiv\text{C}-t\text{-Bu})$) while the remaining Ru–Ru bonds (Ru(1)–Ru(2) 2.8212 (4) vs. 2.792 (1) Å and Ru(1)–Ru(3) 2.8407 (5) vs. 2.799 (1) Å) are quite significantly longer in the substitution product. Thus the increased electron density made available to the skeleton via substitution of a strong π -acceptor ligand, CO, by a stronger σ donor, phosphine, results in a slight but noticeable cluster expansion.

The acetylide is bonded to all three ruthenium atoms in a $\mu_3\text{-}\eta^2$ mode with the σ interaction to Ru(1) and η bonds to Ru(2) and Ru(3). This type of interaction has now been structurally demonstrated for several ruthenium clusters, including the parent $\text{HRu}_3(\text{CO})_9(\text{C}\equiv\text{C}-t\text{-Bu})$,^{13,15} a 2,4-hexadiene reaction product $\text{HRu}_3(\text{CO})_7(\text{C}\equiv\text{C}-t\text{-Bu})(\text{C}_6\text{H}_{10})$,^{3c} the phosphido-bridged compounds $\text{Ru}_3(\text{CO})_9(\text{C}\equiv\text{C}-i\text{-Pr})(\text{PPh}_2)$ and $\text{Ru}_3(\text{CO})_8(\text{C}\equiv\text{C}-t\text{-Bu})(\text{PPh}_2)$,⁶ an osmium analogue $\text{Os}_3(\text{CO})_9(\text{C}\equiv\text{C}-t\text{-Bu})(\text{PPh}_2)$,⁶ and a tetranuclear cluster $\text{Ru}_4(\text{CO})_8(\mu\text{-}\eta^2\text{-C}\equiv\text{C}-t\text{-Bu})(\mu_3\text{-}\eta^2\text{-C}\equiv\text{C}-t\text{-Bu})(\text{PPh}_2)_2\text{-}(\text{Ph}_2\text{PC}\equiv\text{C}-t\text{-Bu})$.¹⁶ In all of these molecules the acetylenic triple bond is lengthened considerably from the value of 1.200 Å in free acetylene with C=C bond lengths lying between 1.28 and 1.32 Å. The C(9)–C(10) distance in $\text{HRu}_3(\text{CO})_8(\text{C}\equiv\text{C}-t\text{-Bu})(\text{PPh}_2\text{OEt})$ (1.321 (6) Å) is not significantly different from the value of 1.315 (3) Å in $\text{HRu}_3(\text{CO})_9(\text{C}\equiv\text{C}-t\text{-Bu})$.¹³

Table IV. Important Bond Lengths (Å) and Bond Angles (Deg) for $\text{HRu}_3(\text{CO})_8(\text{C}_2-t\text{-Bu})(\text{P}(\text{OEt})\text{Ph}_2)$

(i) Skeletal Bond Lengths and Angles			
Bond Lengths			
Ru(1)–Ru(2)	2.8212 (4)	Ru(2)–Ru(3)	2.7988 (5)
Ru(1)–Ru(3)	2.8407 (5)		
Angles			
Ru(1)–Ru(2)–Ru(3)	60.7 (0)	Ru(2)–Ru(1)–Ru(3)	59.2 (0)
Ru(1)–Ru(3)–Ru(2)	60.0 (0)		
(ii) Bond Lengths and Angles at the Acetylide Ligand			
Bond Lengths			
Ru(1)–C(9)	1.946 (4)	Ru(2)–C(10)	2.243 (4)
Ru(2)–C(9)	2.209 (4)	Ru(3)–C(10)	2.252 (4)
Ru(3)–C(9)	2.194 (4)	C(9)–C(10)	1.320 (6)
Angles			
Ru(1)–C(9)–Ru(2)	85.3 (0)	Ru(2)–C(10)–C(9)	71.3 (1)
Ru(1)–C(9)–Ru(3)	86.4 (0)	Ru(3)–C(10)–C(9)	70.4 (1)
Ru(2)–C(9)–Ru(3)	78.9 (0)	Ru(2)–C(10)–C(11)	135.2 (1)
Ru(2)–C(10)–Ru(3)	77.0 (0)	Ru(3)–C(10)–C(11)	134.8 (1)
Ru(1)–C(9)–C(10)	154.5 (1)	C(9)–C(10)–C(11)	140.2 (2)
Ru(2)–C(9)–C(10)	74.2 (1)	C(9)–Ru(2)–C(10)	34.5 (1)
Ru(3)–C(9)–C(10)	75.1 (1)	C(9)–Ru(3)–C(10)	34.5 (1)
(iii) Bond Lengths and Angles at Phosphite and Hydride Ligands			
Bond Lengths			
Ru(2)–H(1)	1.76 (5)	Ru(1)–P	2.294 (1)
Ru(3)–H(1)	1.73 (5)		
Angles			
Ru(2)–H(1)–Ru(3)	106.6 (0)	Ru(2)–Ru(3)–H(1)	37 (2)
Ru(1)–Ru(2)–H(1)	83 (1)	Ru(3)–Ru(2)–H(1)	36 (1)
Ru(1)–Ru(3)–H(1)	82 (2)	Ru(3)–Ru(1)–P	104.0 (0)
Ru(2)–Ru(1)–P	157.4 (0)		
(iv) Other Peripheral Bond Lengths and Angles			
Bond Lengths			
Ru(1)–C(1)	1.872 (4)	Ru(2)–C(5)	1.923 (6)
Ru(1)–C(2)	1.923 (5)	Ru(3)–C(6)	1.892 (6)
Ru(2)–C(3)	1.940 (5)	Ru(3)–C(7)	1.922 (2)
Ru(2)–C(4)	1.897 (5)	Ru(3)–C(8)	1.945 (6)
Angles			
P–Ru(1)–C(1)	92.5 (1)	C(5)–Ru(2)–C(10)	159.2 (1)
P–Ru(1)–C(2)	94.7 (1)	C(5)–Ru(2)–H(1)	87 (2)
Ru(1)–Ru(2)–C(4)	95.1 (1)	C(9)–Ru(2)–H(1)	86 (2)
Ru(1)–Ru(2)–C(5)	83.9 (1)	C(10)–Ru(2)–H(1)	82 (2)
Ru(3)–Ru(2)–C(3)	107.1 (1)	Ru(1)–Ru(2)–C(3)	168.0 (1)
Ru(3)–Ru(2)–C(4)	142.0 (1)	C(7)–Ru(3)–C(8)	101.7 (2)
Ru(3)–Ru(2)–C(5)	111.3 (1)	C(7)–Ru(3)–C(9)	128.3 (1)
C(6)–Ru(3)–C(7)	92.5 (2)	C(7)–Ru(3)–C(10)	159.4 (1)
C(6)–Ru(3)–C(8)	92.9 (2)	C(7)–Ru(3)–H(1)	86 (4)
C(6)–Ru(3)–C(9)	93.8 (1)	C(8)–Ru(3)–C(9)	129.1 (2)
C(6)–Ru(3)–C(10)	99.1 (1)	C(8)–Ru(3)–C(10)	94.7 (2)
C(6)–Ru(3)–H(1)	178 (2)	C(8)–Ru(3)–H(1)	87 (2)
P–Ru(1)–C(9)	106.8 (1)	C(9)–Ru(3)–H(1)	88 (2)
C(1)–Ru(1)–C(2)	95.5 (1)	C(10)–Ru(3)–H(1)	83 (2)
C(1)–Ru(1)–C(9)	106.1 (1)	Ru(2)–Ru(3)–C(6)	144.5 (1)
C(2)–Ru(1)–C(9)	148.5 (1)	Ru(2)–Ru(3)–C(7)	111.0 (1)
C(1)–Ru(1)–Ru(2)	98.8 (1)	Ru(2)–Ru(3)–C(8)	107.2 (1)
C(2)–Ru(1)–Ru(2)	103.5 (1)	Ru(1)–Ru(3)–C(6)	97.7 (1)
C(1)–Ru(1)–Ru(3)	154.2 (1)	Ru(1)–Ru(3)–C(7)	85.1 (1)
C(2)–Ru(1)–Ru(3)	102.6 (1)	Ru(1)–Ru(3)–C(8)	167.1 (1)
C(3)–Ru(2)–C(4)	96.4 (2)	Ru(1)–C(1)–O(1)	177.2 (1)
C(3)–Ru(2)–C(5)	98.6 (2)	Ru(1)–C(2)–O(2)	176.3 (2)
C(3)–Ru(2)–C(9)	132.8 (1)	Ru(2)–C(3)–O(3)	176.9 (2)
C(3)–Ru(2)–C(10)	98.3 (1)	Ru(2)–C(4)–O(4)	177.4 (2)
C(3)–Ru(2)–H(1)	86 (2)	Ru(2)–C(5)–O(5)	177.8 (2)
C(4)–Ru(2)–C(5)	93.1 (2)	Ru(3)–C(6)–O(6)	177.8 (2)
C(4)–Ru(2)–C(10)	96.9 (1)	Ru(3)–C(7)–O(7)	177.9 (2)
C(4)–Ru(2)–H(1)	178 (2)	Ru(3)–C(8)–O(8)	177.8 (2)
C(5)–Ru(2)–C(9)	127.3 (1)		

Moreover, the Ru(1)–C(9) bond length (1.946 (4) Å) is identical with that (1.947 (3) Å) in the parent hydride. Comparison of Ru–C distances from C(9) to Ru(2) and Ru(3)

(13) Catti, M.; Gervasio, G.; Mason, S. A. *J. Chem. Soc., Dalton Trans.* **1977**, 2260.

(14) Churchill, M. R.; Hollander, F. J.; Hutchinson, J. P. *Inorg. Chem.* **1977**, *16*, 2655.

(15) Gervasio, G.; Ferraris, G. *Cryst. Struct. Commun.* **1973**, *3*, 447.

(16) Van Wagner, J.; MacLaughlin, S. A.; Taylor, N. J.; Carty, A. J., to be submitted for publication.

and C(10) to Ru(2) and Ru(3) with corresponding bond lengths for $\text{HRu}_3(\text{CO})_9(\text{C}\equiv\text{C}-t\text{-Bu})$ reveals $\Delta(\text{Ru}-\text{C})$ values of only 0.002 and 0.019 Å for C(9) and 0.025 and 0.019 Å for C(10). Thus the substitution of a carbonyl group by PPh_2OEt has an almost negligible effect on the acetylide-metal interactions. It is thus apparent that phosphine substitution, in this cluster system at least, affects predominantly the metallic skeleton.

Acknowledgment. A.J.C. and E.S. are grateful to NATO for the award of a grant.

Registry No. $\text{HRu}_3(\text{CO})_9(\text{C}_2-t\text{-Bu})(\text{P}(\text{OEt})\text{Ph}_2)$, 79272-81-4.

Supplementary Material Available: A listing of observed and calculated structure factors, Table S1 containing hydrogen atom coordinates, and Table S2 listing additional bond lengths and angles (21 pages). Ordering information is given on any current masthead page.

Contribution from the Department of Chemistry,
Texas A&M University, College Station, Texas 77843

Length of a Tungsten-Phosphine Bond Free of Excessive Steric Interactions: Crystal Structure of $\text{W}(\text{CO})_5\text{P}(\text{CH}_3)_3$

F. Albert Cotton,* Donald J. Darensbourg,
and Brian W. S. Kolthammer

Received June 25, 1981

Although interest in the relationship between structure and reactivity of octahedral complexes containing a mixture of CO and phosphine ligands has led to the determination of a number of crystal structures, the available structural data are still far from complete or comprehensive. Many of the known structures are for polyphosphine species such as *fac*- $\text{Cr}(\text{CO})_3(\text{PET}_3)_3$,¹ *cis*- $\text{Cr}(\text{CO})_2(\text{PH}_3)_4$,² and *cis*- $\{\text{Mn}(\text{CO})_2[\text{P}(\text{OMe})_2\text{Ph}]_4\}\text{PF}_6$,³ in which there are geometrical irregularities caused by steric crowding. We have recently undertaken some systematic studies⁴ of the relationship between the chemical properties of some *cis*- $\text{Mo}(\text{CO})_4\text{L}_2$ ($\text{L} = \text{PR}_3$ or PAR_3) compounds and their structures, including steric interactions. These studies, which have revealed several correlations between structure and reactivity, were facilitated by the ready availability of the compounds in useful crystalline form.

However, in trying to analyze the geometry changes forced upon these complexes by multiple carbonyl substitutions, we find there is a limited base of information available on the structures of monosubstituted derivatives of the type $\text{M}(\text{CO})_5\text{L}$ ($\text{M} = \text{Cr}, \text{Mo}, \text{W}$; $\text{L} = \text{a phosphine}$). This is inherently due to the low melting points of most of these derivatives, which make them unsuitable for X-ray study under normal conditions. Some results have been reported for bulkier phosphine such as PPh_3 and $\text{P}(\text{OPh})_3$ since these give complexes with acceptable physical properties. The majority of these reports deal with chromium compounds such as $\text{Cr}(\text{CO})_5(\text{PPh}_3)$,⁵ $\text{Cr}(\text{CO})_5[\text{P}(\text{OPh})_3]$,⁶ and $\text{Cr}(\text{CO})_5[\text{P}(\text{CH}_3)_2\text{SH}]$.⁶ The

Table I. Crystallographic Data and Enraf-Nonius CAD-4 Data Collection Parameters

formula	$\text{WPO}_5\text{C}_8\text{H}_9$	c , Å	15.479 (2)
mol wt	400.0	β , deg	103.11 (1)
space group	$P2_1/n$	V , Å ³	1278.0 (5)
a , Å	7.134 (1)	Z	4
b , Å	11.882 (2)	d_{calcd} , g/cm ³	2.08
$\mu(\text{Mo K}\alpha)$, cm ⁻¹		96.99	
radiation		graphite-monochromated	
		Mo K α ($\lambda = 0.71073$ Å)	
scan type		$\omega-2\theta$	
scan width ($\Delta\omega$), deg		$0.75 + 0.35 \tan \theta$	
maximum counting time, s		30	
collection range		$+h, +k, \pm l$	
no. of unique data		2228	
no. of data, $I > 3\sigma(I)$		1689	
P		0.05	
no. of variables		136	
R_1^a		0.043	
R_2^a		0.053	
esd		1.62	
largest shift ^b		0.01	
largest peak ^c		0.59	

^a $R_1 = \sum ||F_o| - |F_c|| / \sum |F_o|$; $R_2 = [\sum w(|F_o| - |F_c|)^2 / \sum w|F_o|^2]^{1/2}$. ^b Largest parameter shift in final refinement cycle. ^c Largest peak in a final difference Fourier, e/Å³.

structures of complexes of molybdenum with $\text{L} = \text{PPh}_3$ and $\text{P}(\text{CH}_2\text{CH}_2\text{CN})_3$ have also been published.⁷ The only structural report of a tungsten compound deals with $\text{W}(\text{CO})_5[\text{P}(t\text{-Bu})_3]$.⁸ These derivatives also exhibit some steric interaction between the bulky phosphine ligand and the *cis* carbonyl groups. This is particularly the case in the structure of $\text{W}(\text{CO})_5[\text{P}(t\text{-Bu})_3]$, where these forces are so large that no reliable estimate of a "normal" $\text{W}-\text{PR}_3$ bond length can be obtained.

To obtain structural information for a nondistorted tungsten complex that will provide equilibrium distances mainly determined by electronic factors, we have undertaken an X-ray structural investigation of $\text{W}(\text{CO})_5(\text{PMe}_3)$. We report here the results of this determination and contrast the observed features with those determined for the tri-*tert*-butylphosphine derivative.

Experimental Section

Preparation of $\text{W}(\text{CO})_5(\text{PMe}_3)$. A procedure similar to that described⁹ for other $\text{M}(\text{CO})_5\text{L}$ complexes was employed. A methylene chloride solution (30 mL) containing 0.90 g (1.0 mmol) of $\text{PPN}[\text{W}(\text{CO})_5\text{Cl}]$ and 0.10 mL (0.80 g; 1.1 mmol) of PMe_3 was treated with 10 mL methanol. The mixture was stirred at ambient temperature under nitrogen for 12 h and then filtered through Celite, and volatile materials were removed under reduced pressure. The white residue was then sublimed (45 °C; 10^{-2} torr) to produce crystals of $\text{W}(\text{CO})_5(\text{PMe}_3)$ deemed suitable for X-ray work.

The infrared spectrum in hexane solution has three ν_{CO} bands (each ± 1 cm⁻¹) at 2073, 1952, and 1942 cm⁻¹, corresponding to the $A_1^{(2)}$, $A_1^{(1)}$, and E modes, respectively, of the $\text{W}(\text{CO})_5$ moiety under C_{4v} symmetry.

X-ray Crystallography. A crystal of dimensions $0.20 \times 0.25 \times 0.30$ mm was fixed in a 0.2-mm thin-walled capillary with epoxy cement. The crystal was then mounted on an Enraf-Nonius CAD-4 automated diffractometer where alignment and determination of lattice parameters were performed by using standard routines. The observed cell constants (Table I) and the systematic absences in $h0l$ for $h + l \neq 2n$ and in $0k0$ for $k \neq 2n$ uniquely determined the space group $P2_1/n$.

(1) Halladay, A.; Churchill, M. R.; Wong, A.; Atwood, J. D. *Inorg. Chem.* **1980**, *19*, 2195.

(2) Mattner, G.; Schelle, S. J. *Cryst. Mol. Struct.* **1971**, *1*, 69.

(3) Kruger, G. J.; Heckroodt, R. D.; Reimann, R. H.; Singleton, E. J. *Organomet. Chem.* **1976**, *111*, 225.

(4) Cotton, F. A.; Darensbourg, D. J.; Klein, S.; Kolthammer, B. W. S., submitted for publication in *Inorg. Chem.*

(5) Plastas, M. J.; Stewart, J. M.; Grim, S. O. *J. Am. Chem. Soc.* **1969**, *91*, 4326.

(6) Meier, Von W.-P.; Strahle, J.; Lindner, E. *Z. Anorg. Allg. Chem.* **1976**, *424*, 154.

(7) Cotton, F. A.; Darensbourg, D. J.; Ilsley, W. H. *Inorg. Chem.* **1981**, *20*, 578.

(8) Pickardt, Von J.; Rösch, L.; Schumann, H. *Z. Anorg. Allg. Chem.* **1976**, *426*, 66.

(9) Connor, J. A.; Jones, E. M.; McEwen, G. K. *J. Organomet. Chem.* **1972**, *43*, 357.